Proceedings of the International Conference on Intelligent Data Communication Technologies and Internet of Things (IDCIoT 2023)
IEEE Xplore Part Number: CFP23CV1-ART; ISBN: 978-1-6654-7451-1

2023 International Conference on Intelligent Data Communication Technologies and Internet of Things (IDCIoT) | 978-1-6654-7451-1/23/$31.00 ©2023 IEEE | DOI: 10.1109/IDCIoT56793.2023.10053418

Hyperparameter Tuned Deep Learning Model for Healthcare Monitoring System in Big Data

[1]Dr. Shahnawaz Ayoub
[1]Assistant Professor, Department of Computer Science, Shri Venkateshwara University, Gujrala Amroha, Uttar Pradesh, India, shahnawazayoub@outlook.com

[2]Nihar Ranjan Behera
[2]DBA Researcher, Swiss School of Business and Management Geneva, Av. des Morgines 12, 1213 Petit-Lancy, Switzerland, nihar1773@gmail.com

[3]Meena Naga Raju
*[3]Assistant professor, Department of ECE, Velagapudi Ramakrishna Siddhartha Engineering College, Vijayawada, Andhra Pradesh, India*nagarajumeena@gmail.com

[4]Dr. Pallavi Singh
[4]Assistant Professor, School of Allied Health Sciences, Jaipur National University, Jagatpura, Jaipur, Rajasthan, India. singh.pallavi010@gmail.com

[5]Dr. S. Praveena
[5]Associate professor, MGIT, Department of ECE, Hyderabad, Telangana, India. Spraveena_ece@mgit.ac.on

[6]Ravikiran K
[6]Associate professor, Department of Information Technology, Gokaraju Rangaraju Institute of Engineering and Technology, Hyderabad, Telangana, India. ravi.10541@gmail.com

***Abstract*—Medical image classifiers roles a crucial play in medical service and teaching tasks. But the classical approach obtained its ceiling on performance. Besides, from their use, much longer and more effort require spent on extracted and selected classifier features. The Deep Neural Network (DNN) is a developing Machine Learning (ML) approach which is verified their potential for distinct classifier tasks. Especially, the Convolutional Neural Network (CNN) leads to optimum outcomes on distinct image classifier tasks. But medical image databases can be hard for collecting as it requires several professional skills to categorize them. This study develops a new Hyperparameter Tuned Deep Learning Model for Healthcare Monitoring Systems (HPTDLM-HMS) in big data environment. The presented HPTDLM-HMS technique concentrates on the examination of medical images in the decision-making process. Initially, the presented HPTDLM-HMS technique derives features using EfficientNet model with Manta Ray Foraging Optimization (MRFO) algorithm as hyperparameter tuner. At last, the classification of medical images takes place by Long Short-Term Memory (LSTM) method. To handle big data, Hadoop MapReduce is utilized. The result analysis of the HPTDLM-HMS technique is tested on medical imaging dataset. The comprehensive study of the HPTDLM-HMS technique highlighted and gives recall value of 87.46% is higher when compared to its promising outcomes over other models.**

Keywords*— *Big data; Medical imaging; Manta Ray Foraging Optimization (MRFO); Healthcare monitoring; Deep learning

I. INTRODUCTION

Nowadays, the health care field has seen rapid development in medical data. In the wake of this accumulation of healthcare data, particularly imageries, the usage of novel techniques related to big data technology, Artificial Intelligence (AI), and Machine Learning (ML) has become essential [1]. Big data is usually recognized by 5 major features named the "5V": variability (inconsistency of data), volume (quantity of data produced), variety (data from diverse categories), veracity (quality of captured data), and velocity (rapidity of data production) [2]. The use of information knowledge in the healthcare domain increases the chances for the growth of novel treatments and diagnostics, making it a serious area of study [3]. The novel ideas, technologies, and concepts related to AI, big data, and ML are projected to progress in the healthcare domain. Currently, several works were made to use big data to achieve and study healthcare schemes [4]. Fig. 1 depicts the overview of big data in the healthcare system.

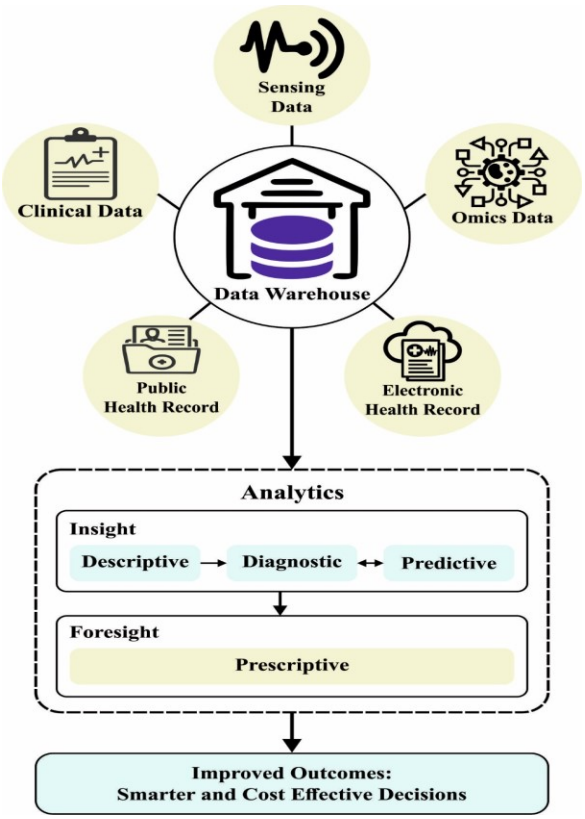

Fig. 1. Big data in healthcare system

Recently, handcrafted feature representatives were commonly utilized in medical sector and several systems have used the union of lower-level features [5]. Lower-level features are gained and assessed with particular structures [6], quality structures, or founded on color structures and many articles to integrate the influential representation of images. These structures are significant for the classification but handcrafted features to preserve consciousness of previous facts [7]. This is difficult task to make the hand-craft structures and wants labelling data for drill and tuning. A data driven technique for classification exploration and image depiction is more vigorous to the variety of image modalities [8]. ML approaches are useful to the lower-level image graphics to do image arrangement. The working refrain of the deep neural networks (DNN) is enthused by the human brain [9]. The DNN design contains many neuron layers. Diverse DL methods are useful in numerous applications for video and image classification like natural language processing, visual tracking, and speech recognition [10].

The authors [11] focused on new IoT application-related physiological signal monitoring scheme to develop e-healthcare system. The presented scheme is prototyped as a progressive electronics factor through an intellectual sensor for signal dimension, National Instrument myRIO for smart data acquisitions. Alfian et al. [12] offer a personalized healthcare monitoring scheme using BLE-related sensors, real-time data processing, and ML–related techniques to aid diabetic patients. BLE is employed for collecting users' vital signs data like weight, blood pressure, blood glucose (BG), and heart rate from SNs.Hossain et al. [13] presented a B5G background that uses the low-latency of 5G networks, and high-bandwidth functionality to distinguish COVID-19 with chest X-ray or CT scan images, to progress a mass surveillance mechanism to observe body temperature, social distancing, and mask wearing. Three DL methods, Inception v3, ResNet50, and Deep tree are examined in the presented structure.

Qi and Su [14] introduced a possible Cybertwin related multimodal network (beyond 5G) for electrocardiogram (ECG) designs monitoring daily activity. The Cybertwin nodes integrate support locators or identifier detection, communications assistant, data caching, and behavior logger in edge cloud. The application emphasizes observing ECG paradigms throughout daily action as some studies analyze them under diverse motions. The author presented a new deep CNN related HAR classifier to improve detection accuracy. Kondaka et al. [15] present a novel method named iCloud Assisted Intensive DL (iCAIDL) that delivers support to healthcare medium along with the patients enforcing the intellectual cloud system with ML approaches and this presented process is extracted from DL norms.

This study develops a new Hyperparameter Tuned Deep Learning Model for Healthcare Monitoring Systems (HPTDLM-HMS) in big data environment. The presented HPTDLM-HMS technique concentrates on the examination of medical images in the decision making process. Initially, the presented HPTDLM-HMS technique derives features using EfficientNet model with manta ray foraging optimization (MRFO) algorithm as hyperparameter tuner. At last, the classification of medical images takes place by long short term memory (LSTM) model. To handle big data, Hadoop Mapreduce is utilized. The result analysis of the HPTDLM-HMS technique is tested on medical imaging dataset. The comprehensive study of the HPTDLM-HMS technique highlighted its promising outcomes over other models.

II. The Proposed Model

In this study, an automated healthcare classification model using HPTDLM-HMS approach was developed in the big data environment. The presented HPTDLM-HMS technique concentrates on the examination of medical images in the decision-making process. Initially, the presented HPTDLM-HMS technique derives features using EfficientNet model with the MRFO algorithm as hyperparameter tuner. At last, the classification of medical images takes place by the LSTM model.

A. EfficientNet Feature Extractor

To create feature vectors, the EfficientNet model is applied. EfficientNet is amongst the most precise approaches (allowing the minimal FLOPS for approximation) that really meet new efficiency through ImageNet and conventional image classification transfer learning objectives [16]. EfficientNet delivers a family of models (BO to B7) which demonstrates the stimulating contrast of accuracy and precision on the array of products by giving a hybrid methodology scaling the model. ImageNet data models have increased extremely vigorously, and because of these accomplished accuracy was improved, even though most inefficient with respect to computation problems. The EfficientNet module might be considered as a collection of CNN approaches because it accomplished maximum accuracy i.e. 84.4% exploiting $66M$ parameter through ImageNet classification tasks. EfficientNet generates rather vigorous outcomes through uniformly intensifying range, sharpness, and density. In the provided resource limitation, the initial stage in the compound scaling method is to find the grid for determining the relationships among the numerous scaling sizes of the baseline network. This technique defines the suitable scaling factors for the depth, breadth, and resolution parameters. The fundamental building element for EfficientNet is the inverted bottleneck MBConv that is firstly presented in MobileNetV2, however, it is slightly applied when compared to $MobileNetV2$ due to the highest FLOPS (floating point operations per second) budget. Block in MBConv is composed of a layer that enlarges and later compresses those channels, thereby direct connection was exploited amongst bottlenecks with significantly reduced channels than that of expansion layer. In comparison with typical layer, this method has depth-wise separable convolution layer which decreases computation by nearly K2 factor whereas k denotes the kernel size that represents the height and width of $2D$ convolutional window.

B. MRFO based Hyperparameter Optimizer

For modifying the hyperparameter values of the EfficientNet method, the MRFO system is exploited. Finally, the MRFO approach is employed as a parameter tuning algorithm. The inspiration for MRFO depends on the smart foraging performance of MR. It takes 3 special foraging rules of manta rays (MR) for detecting the best food source [17]. MRFO is worked by 3 foraging performances as Chain,

Cyclone, and Somersault foraging. Some arithmetical models are shown in the following. When the plankton concentration was improved, then the location is optimum where each position was upgraded by outstanding solution predictable:

$$C_x^{dim}(n+1) = C_x^{dim}(n) + rand.C_{best}^{dim}(n) + \varphi C_{best}^{dim}(n) - C_x^{dim}(n). \quad X = 1 \tag{1}$$

$$C_x^{dim}(n+1) = C_x^{dim}(n) + rand.C_{x-1}^{dim}(n) - C_x^{dim}(n) + \varphi C_{best}^{dim}(n) - C_x^{dim}(n) \quad X = 2 \dots \dots N \tag{2}$$

Whereas, indicates the position of x^{th} individual at time n in dim denotes the dimensional, $rand$ means the arbitrary vector within [0, 1], φ indicates the weighted coefficient, characterizes the plankton with maximum concentration. The mathematical concept of spiral-shaped event of MRs is determined as follows:

$$C_x(n+1) = C_{best} + rand.\left(C_{x-1}(n) - C_x(n) + r^{at}.\cos(2\pi t).\left(C_{best} - C_x(n)\right)\right) \tag{3}$$

$$D_x(n+1) = D_{best} + rand.\left(D_{x-1}(n) - D_x(n) + r^{at}.\cos(2\pi t).\left(D_{best} - D_x(n)\right)\right) \tag{4}$$

These performances are upgraded to d space. The mathematical modelling of cyclone foraging was determined by:

$$C_x^{dim}(n+1) = C_{best}^{dim} + rand.\left(C_{best}^{d}(n) - C_x^{d}(n) + \alpha C_{best}^{dim}(n) - C_x^{dim}(n)\right). \quad X = 1 \tag{5}$$

$$C_x^{dim}(n+1) = C_{best}^{dim} + rand.\left(C_{best}^{d}(n) - C_x^{d}(n) + \alpha C_{best}^{dim}(n) - C_x^{dim}(n)\right). \quad X = 2 \dots \dots N \tag{6}$$

$$A = 2E^{rand1\frac{T-t+1}{T}} \cdot Sin(2\pi rand1) \tag{7}$$

From the expression, α shows the weighted coefficient, T indicates the greater quantity of iterations, and $rand1$ indicates the randomly generated number within [0, 1]. Each individual finds a novel position besides best one by transferring a novel arbitrary location from the search space position.

$$C_r^{dim} = LB^{dim} + rand(UB^{dim} - LB^{dim}) \tag{8}$$

Whereas $rand$ indicates the random location, LB and UB show the lower and upper boundaries. Each MR propose to somersault and move to novel position is given below:

$$C_x^{dim}(n+1) = C_x^{dim}(n) + som.rand2.\left(C_{best}^{dim}(n) - rand3C_x^{dim}(n)\right) \quad X = 1 \dots N \tag{9}$$

In Eq. (9), som indicates the somersault factor which selects a somersault threshold of MR, and *S*om= rand2 and rand3 define 2 random numbers within [0, 1].

The MRFO method designs a fitness function (FF) to realize high classification results. It describes the positive integer to exemplify the best efficiency of candidate result. The reduction classifier error rate was assumed that FF is expressed as follows:

$$fitness(x_i) = ClassifierErrorRate(x_i) = \frac{number\ of\ misclassified\ samples}{Total\ number\ of\ samples} * 100 \tag{10}$$

C. LSTM Classification Model

To identify the class labels, the LSTM model is executed. Hochreiter in 1997 suggested an LSTM network as an enriched RNN for time sequences learning tasks [18]. In comparison with the typical RNN module, LSTM presents a new cell structure that assists in resolving the long- term dependency of time sequence and is appropriate to learn classification from knowledge. The LSTM cell comprises three gates, such forget, output, and input gates. The gate controls the adding or discarding of data to forget or remember functions.

The input gate defines what data from χ_i is stored in the cell state C_t.

$$i_t = \sigma(W_i \cdot [h_{t-1}, x_t] + b_i) \tag{11}$$

$$\tilde{C}_t = \tanh(W_C \cdot [h_{t-1}, x_t] + b_C) \tag{12}$$

From the expression, $\sigma(\cdot)$ denotes a sigmoid function which translates the parameter to a value within [0,1 tanh shows the hyperbolic tangent function that output values within [1, 1]; χ_i indicates the input values at t moment, h_t indicates the hidden layer at t moment, W shows the weight; and b represent the bias. The forget gate determines what data is rejected in cell state. f_t defines what amount of prior cells state C_{t-1} is maintained to the present cell state C_t.

$$f_t = \sigma(W_f \cdot [h_{t-1}, x_t] + b_f) \tag{13}$$

$$C_t = f_t * C_{t-1} + i_t * \tilde{C}_t \tag{14}$$

The output gate is used for controlling what amount of data is filtered out in the new state C_t.

$$0_t = f(W_0 \cdot [h_{t-1}, x_t] + b_0) \tag{15}$$

$$h_t = 0_t * \tanh(C_t) \tag{16}$$

III. Results and Discussion

In this section, the experimental results of the HPTDLM-HMS technique are tested using a dataset including 7200 samples with 12 classes as given in Table 1.

TABLE I

DETAILS OF DATASET

Label	Class	No. of Images
C-1	Brain	600
C-2	Breast	600
C-3	Chest	600
C-4	Bladder	600
C-5	Colon	600
C-6	Cervix	600
C-7	Eye	600
C-8	Esophagus	600
C-9	Lymph	600
C-10	Pancreas	600
C-11	Prostate	600
C-12	Soft Tissue	600
Total Number of Images		**7200**

The confusion matrices of the HPTDLM-HMS technique on healthcare data classification are reported in Fig. 2. The results indicated that the HPTDLM-HMS technique has identified distinct classes.

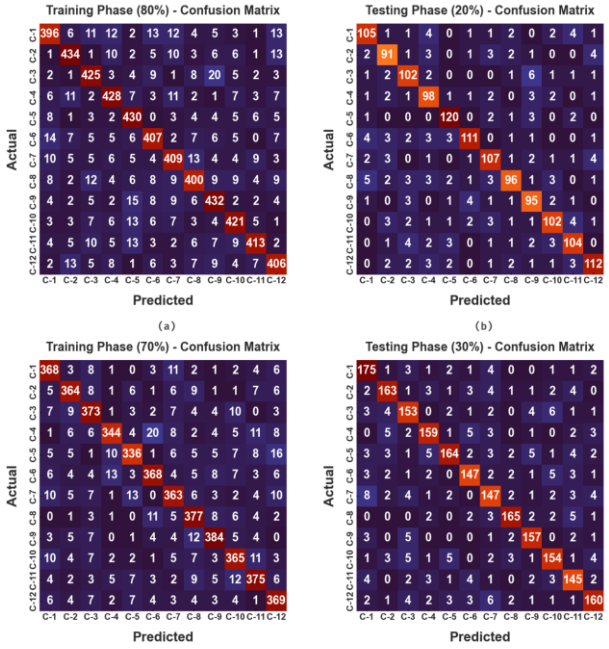

Fig. 2. Confusion matrices of HPTDLM-HMS approach (a-b) TRS and TSS databases of 80:20 and (c-d) TRS and TSS databases of 70:30

In Table 2 and Fig. 3, the experimental results of the HPTDLM-HMS technique is examined on 80:20 of TRS and TSS. With 80% of TRS, the HPTDLM-HMS technique has recognized C-1 samples with $accu_y$ of 97.50%, $prec_n$ of 86.46%, $rec a_l$ of 82.85%, F_{score} of 84.62%, and MCC of 83.28%. In line with, with 80% of TRS, the HPTDLM-HMS system has recognized C-5 samples with $accu_y$ of 98%, $prec_n$ of 85.32%, $rec a_l$ of 91.30%, F_{score} of 88.21%, and MCC of 87.18%. Next, with 80% of TRS, the HPTDLM-HMS approach has recognized C-12 samples with $accu_y$ of 97.71%, $prec_n$ of 85.84%, $rec a_l$ of 86.20%, F_{score} of 86.02%, and MCC of 84.77%. Then, with 20% of TSS, the HPTDLM-HMS methodology has recognized C-1 samples with $accu_y$ of 97.64%, $prec_n$ of 86.07%, $rec a_l$ of 86.07%, F_{score} of 86.07%, and MCC of 84.78%. At last, with 20% of TSS, the HPTDLM-HMS algorithm has recognized C-12 samples with $accu_y$ of 97.85%, $prec_n$ of 88.89%, $rec a_l$ of 86.82%, F_{score} of 87.84%, and MCC of 86.67%.

TABLE II

RESULT ANALYSIS OF HPTDLM-HMS SYSTEM WITH DISTINCT CLASSES ON 80:20 OF TRS/TSS

Labels	Accuracy	Precision	Recall	F-Score	MCC
Training Phase (80%)					
C-1	97.50	86.46	82.85	84.62	83.28
C-2	98.02	88.57	88.21	88.39	87.31
C-3	97.85	86.56	87.99	87.27	86.10
C-4	97.86	87.17	87.70	87.44	86.27
C-5	98.00	85.32	91.30	88.21	87.18
C-6	97.76	86.23	86.41	86.32	85.10
C-7	97.62	85.56	85.74	85.65	84.36
C-8	97.52	86.39	83.33	84.84	83.50
C-9	97.67	85.21	87.98	86.57	85.31
C-10	97.97	87.71	87.89	87.80	86.69
C-11	98.16	91.17	86.22	88.63	87.67
C-12	97.71	85.84	86.20	86.02	84.77
Average	**97.80**	**86.85**	**86.82**	**86.81**	**85.63**
Testing Phase (20%)					
C-1	97.64	86.07	86.07	86.07	84.78
C-2	97.50	82.73	84.26	83.49	82.14
C-3	97.64	84.30	87.18	85.71	84.44
C-4	97.50	81.67	87.50	84.48	83.18
C-5	98.47	90.23	93.02	91.60	90.78
C-6	97.99	90.98	86.05	88.45	87.38
C-7	97.71	86.29	86.99	86.64	85.39
C-8	97.43	88.07	80.00	83.84	82.56
C-9	97.57	81.90	87.16	84.44	83.17
C-10	97.64	87.18	84.30	85.71	84.44
C-11	97.71	86.67	85.95	86.31	85.06
C-12	97.85	88.89	86.82	87.84	86.67
Average	**97.72**	**86.25**	**86.27**	**86.22**	**85.00**

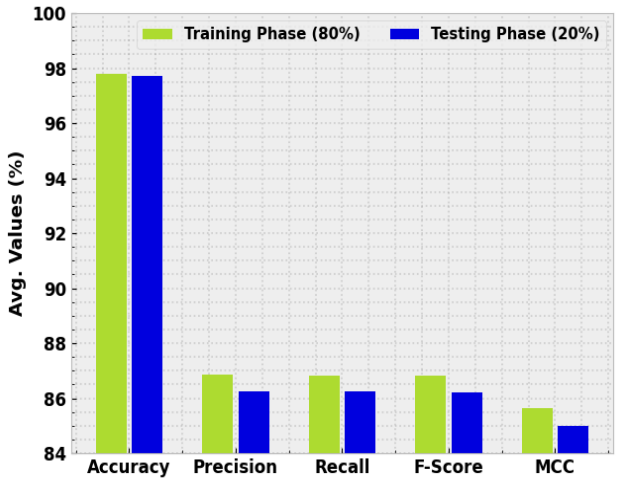

Fig. 3. Average analysis of HPTDLM-HMS system on 80:20 of TRS/TSS

In Table 3 and Fig. 4, the experimental outcomes of the HPTDLM-HMS approach are examined on 70:30 of TRS and TSS. With 70% of TRS, the HPTDLM-HMS methodology has recognized C-1 samples with $accu_y$ of 98.06%, $prec_n$ of 86.59%, $rec a_l$ of 89.98%, F_{score} of 88.25%, and MCC of 87.21%. Likewise, with 70% of TRS, the HPTDLM-HMS algorithm has recognized C-5 samples with $accu_y$ of 97.72%, $prec_n$ of 87.96%, $rec a_l$ of 82.96%, F_{score} of 85.39%, and MCC of 84.19%. Followed by, with 70% of TRS, the HPTDLM-HMS technique has recognized C-12 samples with $accu_y$ of 97.80%, $prec_n$ of 84.83%, $rec a_l$ of 89.13%, F_{score} of 86.93%, and MCC of 85.76%. Afterward, with 30% of TSS, the HPTDLM-HMS methodology has recognized C-1 samples with $accu_y$ of 97.92%, $prec_n$ of 85.78%, $rec a_l$ of 91.62%, F_{score} of 88.61%, and MCC of 87.52%. Finally, with 30% of TSS, the HPTDLM-HMS system has recognized C-12 samples with $accu_y$ of 97.82%, $prec_n$ of 88.40%, $rec a_l$ of 86.02%, F_{score} of 87.19%, and MCC of 86.01%.

TABLE III

RESULT ANALYSIS OF HPTDLM-HMS SYSTEM WITH DISTINCT CLASSES ON 70:30 OF TRS/TSS

Labels	Accuracy	Precision	Recall	F-Score	MCC
Training Phase (70%)					
C-1	98.06	86.59	89.98	88.25	87.21
C-2	98.04	88.35	87.71	88.03	86.96
C-3	97.80	85.94	88.18	87.05	85.85
C-4	97.78	90.29	82.10	86.00	84.91
C-5	97.72	87.96	82.96	85.39	84.19
C-6	97.76	88.04	85.38	86.69	85.48
C-7	97.58	85.61	85.61	85.61	84.29
C-8	97.90	85.29	90.19	87.67	86.57
C-9	98.21	89.51	89.51	89.51	88.53
C-10	97.70	85.68	86.90	86.29	85.03
C-11	97.72	86.81	86.61	86.71	85.46
C-12	97.80	84.83	89.13	86.93	85.76
Average	**97.84**	**87.07**	**87.02**	**87.01**	**85.85**
Testing Phase (30%)					
C-1	97.92	85.78	91.62	88.61	87.52
C-2	98.01	88.59	88.11	88.35	87.26
C-3	97.59	84.53	86.44	85.47	84.17
C-4	98.06	88.83	87.85	88.33	87.27
C-5	97.78	90.61	84.10	87.23	86.09
C-6	98.01	87.50	86.98	87.24	86.16
C-7	97.22	82.58	83.52	83.05	81.54
C-8	98.56	92.18	90.66	91.41	90.63
C-9	98.47	89.20	91.81	90.49	89.67
C-10	97.73	87.01	85.56	86.27	85.04
C-11	97.73	84.30	86.83	85.55	84.33
C-12	97.82	88.40	86.02	87.19	86.01
Average	**97.91**	**87.46**	**87.46**	**87.43**	**86.31**

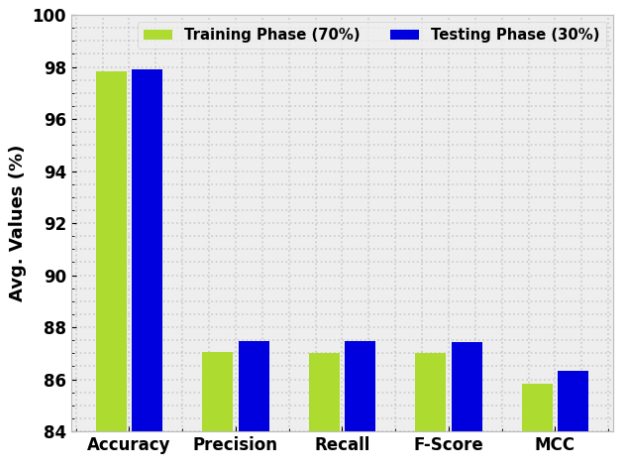

Fig. 4. Average analysis of HPTDLM-HMS system on 70:30 of TRS/TSS

The TACC and VACC of the HPTDLM-HMS approach are investigated performance in Fig. 5. The figure stated that the HPTDLM-HMS system has shown improved performance with increased values of TACC and VACC. It is noticeable that the HPTDLM-HMS methodology has reached maximum TACC outcomes.

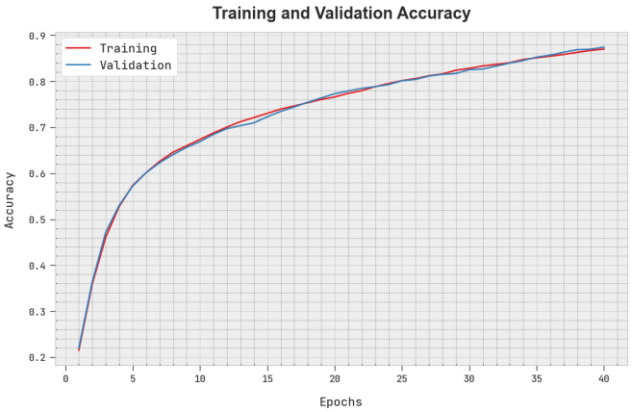

Fig. 5. TACC and VACC analysis of HPTDLM-HMS system

The TLS and VLS of the HPTDLM-HMS system are tested performance in Fig. 6. The figure implied that the HPTDLM-HMS method has revealed better performance with least values of TLS and VLS. It is observable that the HPTDLM-HMS system has resulted in lesser VLS outcomes.

Fig. 6. TLS and VLS analysis of HPTDLM-HMS system

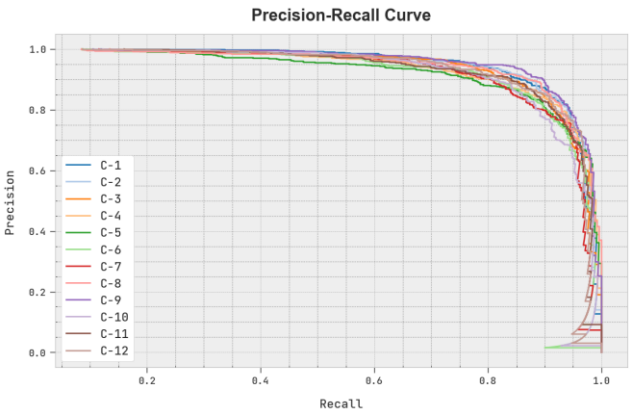

Fig. 7. Precision-recall analysis of HPTDLM-HMS system

A noticeable precision-recall study of the HPTDLM-HMS system in the test database is revealed in Fig. 7. The figure referred that the HPTDLM-HMS algorithm has resulted in superior values of precision-recall values in several classes.

A detailed ROC study of the HPTDLM-HMS system in the test database is described in Fig. 8. The outcome implied the

HPTDLM-HMS algorithm has exhibited its capability in classifying in several classes.

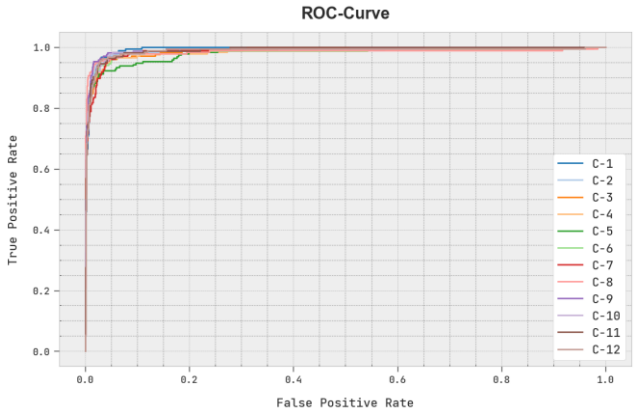

Fig. 8. ROC analysis of HPTDLM-HMS system

The healthcare monitoring performance of the HPTDLM-HMS technique is compared with existing models in Table 4 and Fig. 9 [19]. The experimental output pointed out that the HPTDLM-HMS technique has reached improved performance. Based on $accu_y$, the HPTDLM-HMS technique has gained $accu_y$ of 97.91% while the ANN, SVM, LDA, KELM, and DenseNet models have reached reduced $accu_y$ of 92.38%, 96.93%, 90.73%, 94.80%, and 94.10% respectively. Meanwhile, with respect to $prec_n$, the HPTDLM-HMS technique has gained $prec_n$ of 87.46% while the ANN, SVM, LDA, KELM, and DenseNet techniques have reached minimal $prec_n$ of 86.85%, 85.47%, 83.24%, 86.79%, and 84.79% respectively. At last, interms of $reca_l$, the HPTDLM-HMS technique has gained $reca_l$ of 87.46% while the ANN, SVM, LDA, KELM, and DenseNet systems have gained lesser $reca_l$ of 83.96%, 83.46%, 83.25%, 83.14%, and 84.24% correspondingly.

TABLE IV

COMPARATIVE ANALYSIS OF HPTDLM-HMS SYSTEM WITH OTHER EXISTING METHODS

Methods	Accuracy	Precision	Recall	F-Score
HPTDLM-HMS	97.91	87.46	87.46	87.43
ANN Model	92.38	86.85	83.96	85.78
SVM Model	96.93	85.47	83.46	86.44
LDA Model	90.73	83.24	83.25	86.52
KELM Model	94.80	86.79	83.14	85.25
DenseNet Model	94.10	84.79	84.24	85.44

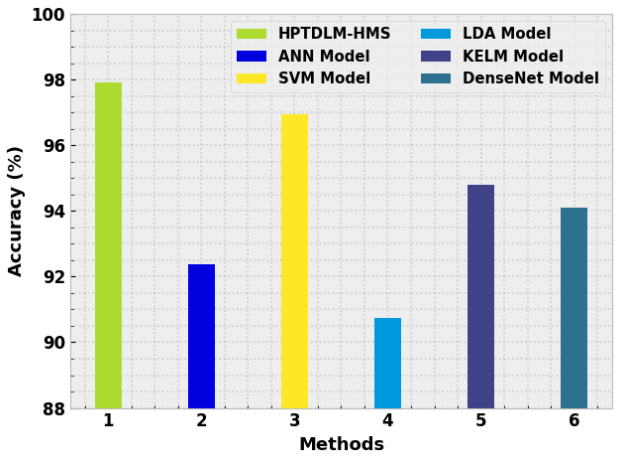

Fig. 9. $Accu_y$ analysis of HPTDLM-HMS system with other existing methods

IV. CONCLUSION

In this study, an automated healthcare classification model using HPTDLM-HMS technique has been developed in the big data environment. The presented HPTDLM-HMS technique concentrates on the examination of medical images in the decision-making process. Initially, the presented HPTDLM-HMS technique derives features using EfficientNet model with the MRFO algorithm as hyperparameter tuner. At last, the classification of medical images takes place by the LSTM model. To handle big data, Hadoop MapReduce is utilized. The result analysis of the HPTDLM-HMS technique is tested on medical imaging dataset. The comprehensive study of the HPTDLM-HMS technique highlighted its promising outcomes over other models. In future, ensemble learning techniques can be integrated into the HPTDLM-HMS technique to boost the predictive outcomes.

REFERENCES

[1] Awotunde, J.B., Jimoh, R.G., Ogundokun, R.O., Misra, S. and Abikoye, O.C., 2022. Big data analytics of iot-based cloud system framework: Smart healthcare monitoring systems. In *Artificial Intelligence for Cloud and Edge Computing* (pp. 181-208). Springer, Cham.

[2] Li, W., Chai, Y., Khan, F., Jan, S.R.U., Verma, S., Menon, V.G. and Li, X., 2021. A comprehensive survey on machine learning-based big data analytics for IoT-enabled smart healthcare system. *Mobile Networks and Applications*, *26*(1), pp.234-252.

[3] Venkatachalam, K., Prabu, P., Alluhaidan, A.S., Hubálovský, S. and Trojovský, P., 2022. Deep belief neural network for 5G diabetes monitoring in big data on edge IoT. *Mobile Networks and Applications*, pp.1-10.

[4] Rashid, M., Singh, H., Goyal, V., Parah, S.A. and Wani, A.R., 2021. Big data based hybrid machine learning model for improving performance of medical Internet of Things data in healthcare systems. In *Healthcare Paradigms in the Internet of Things Ecosystem* (pp. 47-62). Academic Press.

[5] Karatas, M., Eriskin, L., Deveci, M., Pamucar, D. and Garg, H., 2022. Big Data for Healthcare Industry 4.0: Applications, challenges and future perspectives. *Expert Systems with Applications*, p.116912.

[6] Ali, F., El-Sappagh, S., Islam, S.R., Ali, A., Attique, M., Imran, M. and Kwak, K.S., 2021. An intelligent healthcare monitoring framework using wearable sensors and social networking data. *Future Generation Computer Systems*, *114*, pp.23-43.

[7] Verma, P., Tiwari, R., Hong, W.C., Upadhyay, S. and Yeh, Y.H., 2022. FETCH: A Deep Learning-Based Fog Computing and IoT Integrated Environment for Healthcare Monitoring and Diagnosis. *IEEE Access*, *10*, pp.12548-12563.

[8] Harimoorthy, K. and Thangavelu, M., 2021. Multi-disease prediction model using improved SVM-radial bias technique in healthcare monitoring system. *Journal of Ambient Intelligence and Humanized Computing*, *12*(3), pp.3715-3723.

[9] Souri, A., Ghafour, M.Y., Ahmed, A.M., Safara, F., Yamini, A. and Hoseyninezhad, M., 2020. A new machine learning-based healthcare monitoring model for student's condition diagnosis in Internet of Things environment. *Soft Computing*, *24*(22), pp.17111-17121.

[10] Motwani, A., Shukla, P.K. and Pawar, M., 2020, May. Smart predictive healthcare framework for remote patient monitoring and recommendation using deep learning with novel cost optimization. In *International Conference on Information and Communication Technology for Intelligent Systems* (pp. 671-682). Springer, Singapore.

[11] Rajan Jeyaraj, P. and Nadar, E.R.S., 2022. Smart-monitor: patient monitoring system for IoT-based healthcare system using deep learning. *IETE Journal of Research*, *68*(2), pp.1435-1442.

[12] Alfian, G., Syafrudin, M., Ijaz, M.F., Syaekhoni, M.A., Fitriyani, N.L. and Rhee, J., 2018. A personalized healthcare monitoring system for diabetic patients by utilizing BLE-based sensors and real-time data processing. *Sensors*, *18*(7), p.2183.

[13] Hossain, M.S., Muhammad, G. and Guizani, N., 2020. Explainable AI and mass surveillance system-based healthcare framework to combat COVID-I9 like pandemics. *IEEE Network*, *34*(4), pp.126-132.

[14] Qi, W. and Su, H., 2022. A cybertwin based multimodal network for ecg patterns monitoring using deep learning. *IEEE Transactions on Industrial Informatics*.

[15] Kondaka, L.S., Thenmozhi, M., Vijayakumar, K. and Kohli, R., 2022. An intensive healthcare monitoring paradigm by using IoT based machine learning strategies. *Multimedia Tools and Applications*, *81*(26), pp.36891-36905.

[16] SHARMA, P. and SHUKLA, A.P., 2022. TRANSFER LEARNING APPROACH USING EFFICIENTNET ARCHITECTURE FOR BRAIN TUMOR CLASSIFICATION IN MRI IMAGES.

[17] Houssein, E.H., Ibrahim, I.E., Neggaz, N., Hassaballah, M. and Wazery, Y.M., 2021. An efficient ECG arrhythmia classification method based on Manta ray foraging optimization. *Expert Systems with Applications*, *181*, p.115131.

[18] Chen, Y., Xia, W., Chen, D., Zhang, T., Song, T., Zhao, W. and Song, K., 2022. A Qualitative and Quantitative Analysis Strategy for Continuous Turbulent Gas Mixture Monitoring. *Chemosensors*, *10*(12), p.499.

[19] Dharangan, B., Praveen, J., Rajagopal, S., & Jegajothi, B. (2022, August). Secure Cloud-based E-Health System using Advanced Encryption Standard. In *2022 3rd International Conference on Electronics and Sustainable Communication Systems (ICESC)* (pp. 642-646). IEEE.